Atomic Oxygen Erosion Data From the MISSE 2–8 Missions

Kim K. de Groh
Glenn Research Center, Cleveland, Ohio

Bruce A. Banks
Science Applications International Corporation, Cleveland, Ohio

NASA STI Program . . . in Profile

Since its founding, NASA has been dedicated to the advancement of aeronautics and space science. The NASA Scientific and Technical Information (STI) Program plays a key part in helping NASA maintain this important role.

The NASA STI Program operates under the auspices of the Agency Chief Information Officer. It collects, organizes, provides for archiving, and disseminates NASA's STI. The NASA STI Program provides access to the NASA Technical Report Server—Registered (NTRS Reg) and NASA Technical Report Server—Public (NTRS) thus providing one of the largest collections of aeronautical and space science STI in the world. Results are published in both non-NASA channels and by NASA in the NASA STI Report Series, which includes the following report types:

- TECHNICAL PUBLICATION. Reports of completed research or a major significant phase of research that present the results of NASA programs and include extensive data or theoretical analysis. Includes compilations of significant scientific and technical data and information deemed to be of continuing reference value. NASA counter-part of peer-reviewed formal professional papers, but has less stringent limitations on manuscript length and extent of graphic presentations.

- TECHNICAL MEMORANDUM. Scientific and technical findings that are preliminary or of specialized interest, e.g., "quick-release" reports, working papers, and bibliographies that contain minimal annotation. Does not contain extensive analysis.

- CONTRACTOR REPORT. Scientific and technical findings by NASA-sponsored contractors and grantees.

- CONFERENCE PUBLICATION. Collected papers from scientific and technical conferences, symposia, seminars, or other meetings sponsored or co-sponsored by NASA.

- SPECIAL PUBLICATION. Scientific, technical, or historical information from NASA programs, projects, and missions, often concerned with subjects having substantial public interest.

- TECHNICAL TRANSLATION. English-language translations of foreign scientific and technical material pertinent to NASA's mission.

For more information about the NASA STI program, see the following:

- Access the NASA STI program home page at http://www.sti.nasa.gov

- E-mail your question to help@sti.nasa.gov

- Fax your question to the NASA STI Information Desk at 757-864-6500

- Telephone the NASA STI Information Desk at 757-864-9658

- Write to:
  NASA STI Program
  Mail Stop 148
  NASA Langley Research Center
  Hampton, VA 23681-2199

Atomic Oxygen Erosion Data From the MISSE 2–8 Missions

Kim K. de Groh
Glenn Research Center, Cleveland, Ohio

Bruce A. Banks
Science Applications International Corporation, Cleveland, Ohio

National Aeronautics and
Space Administration

Glenn Research Center
Cleveland, Ohio 44135

May 2019

Acknowledgments

Level of Review: This material has been technically reviewed by technical management.

Available from

NASA STI Program
Mail Stop 148
NASA Langley Research Center
Hampton, VA 23681-2199

National Technical Information Service
5285 Port Royal Road
Springfield, VA 22161
703-605-6000

This report is available in electronic form at http://www.sti.nasa.gov/ and http://ntrs.nasa.gov/

Atomic Oxygen Erosion Data From the MISSE 2–8 Missions

Kim K. de Groh
National Aeronautics and Space Administration
Glenn Research Center
Cleveland, Ohio 44135

Bruce A. Banks
Science Applications International Corporation
Cleveland, Ohio 44135

Summary

Polymers and other oxidizable materials on the exterior of spacecraft in the low Earth orbit (LEO) space environment can be eroded from reaction with atomic oxygen (AO). Therefore, in order to design durable spacecraft it is important to know the extent of erosion that will occur during a mission. This can be determined by knowing the LEO AO erosion yield, E_y (volume loss per incident oxygen atom), of materials susceptible to AO reaction. In addition, recent flight experiments have shown that the AO E_y can vary with the AO fluence and/or solar exposure. Therefore obtaining AO E_y data for materials flown on various spaceflight missions is important. NASA Glenn Research Center has flown numerous experiments as part of the Materials International Space Station Experiment (MISSE) missions on the exterior of the International Space Station to characterize the LEO E_y of polymers, composites, protective coatings, and other spacecraft materials. This report provides a summary of the erosion data for ram samples from six Glenn polymer experiments flown as part of MISSE 2, 4, 6, 7, and 8. A total of 71 types of materials with 111 E_y values are provided. The E_y values for uncoated polymers range from 3.81×10^{-27} cm^3/atom for DC 93-500 silicone exposed to an AO fluence of 4.62×10^{21} atoms/cm^2 on MISSE 8 to 9.14×10^{-24} cm^3/atom for polyoxymethylene (POM) exposed to an AO fluence of 8.43×10^{21} atoms/cm^2 on MISSE 2. One polymer, Triton oxygen resistant, low modulus (TOR^{TM} LM), experienced mass gain when exposed to an AO fluence of 2.15×10^{21} atoms/cm^2 on MISSE 4. In many cases the same material was flown on numerous missions so that trends for E_y versus AO fluence and/or solar exposure can be determined, along with temperature effects.

Introduction

Materials used on the exterior of spacecraft are subjected to many environmental threats that can cause degradation. In low Earth orbit (LEO) these threats include photon radiation, ultraviolet (UV) radiation, vacuum ultraviolet (VUV) radiation, x-rays, solar wind particle radiation (electrons, protons), cosmic rays, temperature extremes, thermal cycling, impacts from micrometeoroids and orbital debris (MMOD), spacecraft self-contamination, and atomic oxygen (AO). Although all of these environmental exposures can cause degradation to spacecraft components, AO is a particularly serious structural, thermal, and optical threat, especially to exterior oxidizable spacecraft components.

Atomic oxygen is formed in the LEO environment through photodissociation of diatomic oxygen (O_2). Short-wavelength (<243 nm) solar radiation has sufficient energy to break the 5.12-eV O_2 diatomic bond in an environment where the mean free path is sufficiently long (~10^8 m) so that the probability of re-association, or the formation of ozone (O_3), is small.[1,2] In LEO, between the altitudes of 180 and 650 km, AO is the most abundant species.[3]

A number of processes can take place when an oxygen atom strikes a spacecraft surface as a result of its orbital velocity and the thermal velocity of the atoms. These include chemical reaction with surface molecules, elastic scattering, scattering with partial or full thermal accommodation, and recombination or excitation of ram species, which consists predominantly of ground-state O(^{3}P) atomic oxygen atoms.[4]
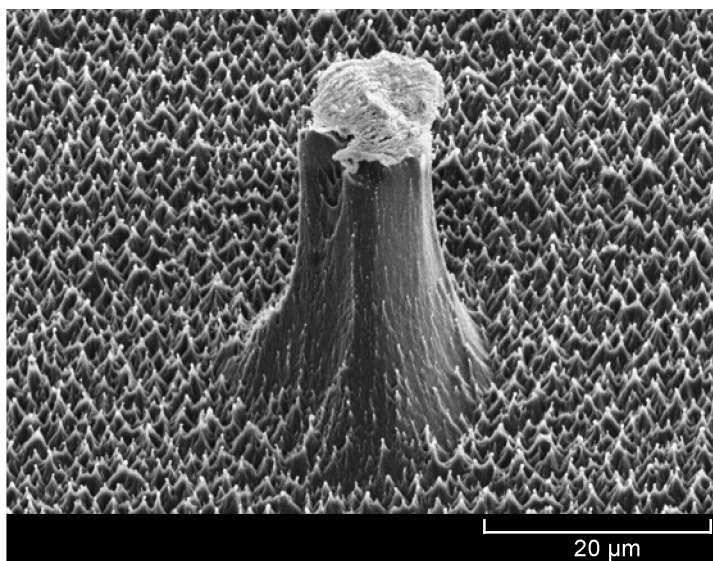
Figure 1.—Atomic oxygen erosion of Teflon™ FEP after 5.8 years of space exposure.

Atomic oxygen can react with polymers, carbon, and many metals to form oxygen bonds with atoms on the exposed surface. For most polymers, hydrogen abstraction, oxygen addition, or oxygen insertion can occur, with the oxygen interaction pathways eventually leading to volatile oxidation products.[5,6] This results in gradual erosion of hydrocarbon or halocarbon material, with the exception of silicone materials, which form a glassy silicate surface layer with AO exposure. Figure 1 shows AO erosion of Teflon™ (The Chemours Company) fluorinated ethylene propylene (FEP) around a small protective particle after 5.8 years of space exposure on the Long Duration Exposure Facility (LDEF). An example of the complete loss of a Kapton® H (E. I. du Pont de Nemours and Company) thermal blanket insulation layer on the LDEF, as well as degradation of other polymeric materials caused by AO erosion in LEO, is provided in Figure 2.[7]

The most common approach to protecting susceptible spacecraft materials from AO erosion is to coat the material with a thin protective film, such as SiO_x (where x = 1.8 to 2). Even materials with AO protective coatings can be susceptible to AO erosion as a result of microscopic scratches, dust particles, or other imperfections in the substrate surface, which can result in defects or pin windows in the protective coating.[8,9] These coating defects can provide pathways for AO attack, and undercutting erosion of the substrate can occur, even under directed ram AO exposure in LEO. One of the first examples of directed ram AO undercutting erosion in LEO was reported by de Groh and Banks for aluminized-Kapton® insulation blankets from the LDEF.[8] Undercutting erosion can be a serious threat to component survivability. An example is shown in Figure 3, where AO undercutting erosion has severely degraded the P6 Truss port solar array wing two-surface aluminized-Kapton® blanket box cover on the International Space Station (ISS) after 1 year of space exposure.

The sensitivity of a hydrocarbon or halocarbon material to react with AO is quantified by the AO erosion yield, E_y, of the material. The AO E_y is the volume of a material that is removed (through oxidation) per incident oxygen atom and is measured in units of cm^3/atom. As AO erosion in LEO is a serious threat to spacecraft performance and durability, it is essential to know the LEO AO E_y so that the durability of materials being considered for spacecraft design can be predicted. The most characterized AO E_y is that of polyimide Kapton® H, which has an E_y of $3.0\pm0.07\times10^{-24}$ cm^3/atom for LEO 4.5-eV AO.[11–14]

Hydrocarbon or halocarbon polymers that contain metal oxide pigment particles, or ash, will have E_y values that are fluence dependent. This is because AO will erode the polymer content on the surface, leaving a proliferation of inorganic particles that tend to shield the underlying polymer from AO attack. As a result, the E_y of the polymer gradually reduces with fluence. In addition, for any particular ash-filled polymer, the greater the volume fill of the ash particles, the greater the rate of reduction in the E_y with fluence.[15]
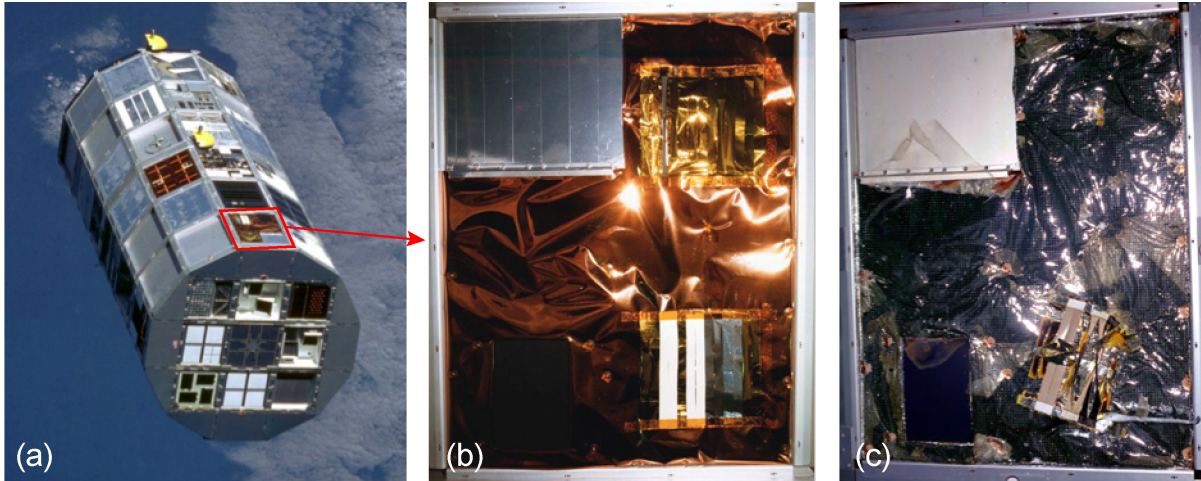
Figure 2.—Atomic oxygen erosion of a Kapton® insulation blanket from LDEF experiment Tray F-9, located on the leading edge and exposed to direct-ram AO for 5.8 years.[7] (a) LDEF. (b) Tray F-9 pre-flight. (c) Tray F-9 post-flight.
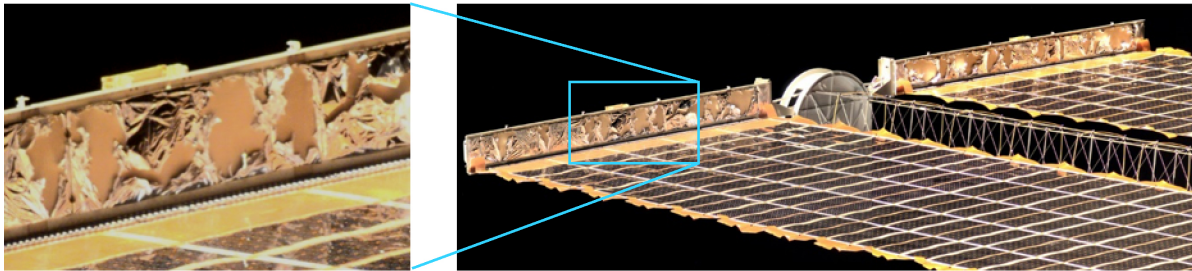

Figure 3.—Atomic oxygen undercutting degradation of the P6 Truss solar array wing blanket box cover on the ISS after only 1 year of space exposure.[10]

Another LEO threat to spacecraft materials is solar UV radiation, which has a typical wavelength of 0.1 to 0.4 μm.[16] Ultraviolet radiation is energetic enough to cause the breaking of organic bonds such as C=C, C=O, and C–H as well as bonds in other functional groups.[5] A molecule is raised to an excited state when an organic molecule absorbs a photon of UV radiation, and bond dissociation can occur if the molecule acquires enough energy at the excited state. Depending on the temperature and physical properties of the materials, the dissociated radical species are reactive intermediates, with the capability of diffusing several atomic distances from their point of origin and can participate in further reactions.[5] Solar radiation often results in bond breakage in materials as well as threats to functionality and stability of the materials. Therefore, solar radiation can impact the erosion of some materials.

Because spaceflight materials exposure opportunities are rare, expensive, space-limited, and time-consuming, ground laboratory testing is often relied upon for spacecraft material environmental durability prediction. However, differences exist between ground facilities and actual space exposures, which may result in differences in rates of oxidation that are material dependent. Therefore, actual spaceflight AO E_y data are needed to best assess the durability of a material for spacecraft mission applicability. In addition, data from actual materials spaceflight experiments can be used to determine correlations between exposures in ground test facilities and space exposure, allowing for more accurate predictions of in-space materials performance based on ground facility testing. Materials spaceflight experiments for E_y determination have been flown on the space shuttle, the LDEF, the Russian space station Mir, and other spacecraft.[17] More recently, experiments have been flown as a part of the Materials International Space Station Experiment (MISSE) missions flown on the exterior of the ISS.[9,17]

To further increase understanding of the AO erosion of spacecraft materials, NASA Glenn Research Center has developed and flown a series of experiments as part of the MISSE 1–8 missions.[9,18–23] This report provides an overview of the MISSE missions, a list of the experiments flown along with pre-flight and post-flight characterization techniques used, the AO fluence and solar exposure for the experiments, and the AO E_y results for samples flown in the ram flight orientation. A total of 71 types of materials with 111 E_y values are summarized from five MISSE missions. The majority of materials are polymers, but other materials such as various forms of carbon (i.e., pyrolytic graphite (PG) and diamond), composites, and protective coatings are included also. The E_y data from these MISSE spaceflight experiments provide valuable information necessary for durable LEO spacecraft design.

Materials International Space Station Experiment (MISSE) Overview

The MISSE program involves is a series of spaceflight missions with experiments flown on the exterior of the ISS to test the performance and durability of materials and devices exposed to the LEO space environment. In the MISSE 1–8 missions, individual flight experiments were flown in suitcase-like containers called Passive Experiment Containers (PECs) that provide exposure to the space environment. The PECs were closed during launch on a shuttle mission to protect the samples. Once on orbit, the PECs were placed on the exterior of the ISS during an extravehicular activity (EVA), or spacewalk, in either a ram/wake or a zenith/nadir orientation and opened, exposing the experiments to the space environment for the duration of the mission. A diagram showing ram, wake, zenith, and nadir directions on the ISS is shown in Figure 4. The flight orientation highly affects the environmental exposure. Ram facing experiments receive a high flux of directed AO and sweeping (moderate) solar exposure. Zenith facing experiments receive a low flux of grazing arrival AO and the highest solar exposure. Wake experiments receive essentially no AO flux and moderate solar radiation (levels similar to ram experiments). Nadir experiments receive a low flux of grazing arrival AO and minimal solar radiation (albedo sunlight). All surfaces receive charged particle and cosmic radiation, which are omnidirectional. It should be noted that the actual orientation of the ISS varies because of operational requirements with the majority of the time spent within ±15° of the +XVV Z nadir flight attitude, defined as[24] the "+X axis aligned toward the Velocity Vector (VV) and the +Z axis aligned towards the Nadir." Deviations from this attitude to accommodate visiting spacecraft, and other ISS operational needs, can cause variations in the orientation directions, and hence variations in environmental exposures especially for atomic oxygen exposure of zenith, nadir, and wake surfaces.
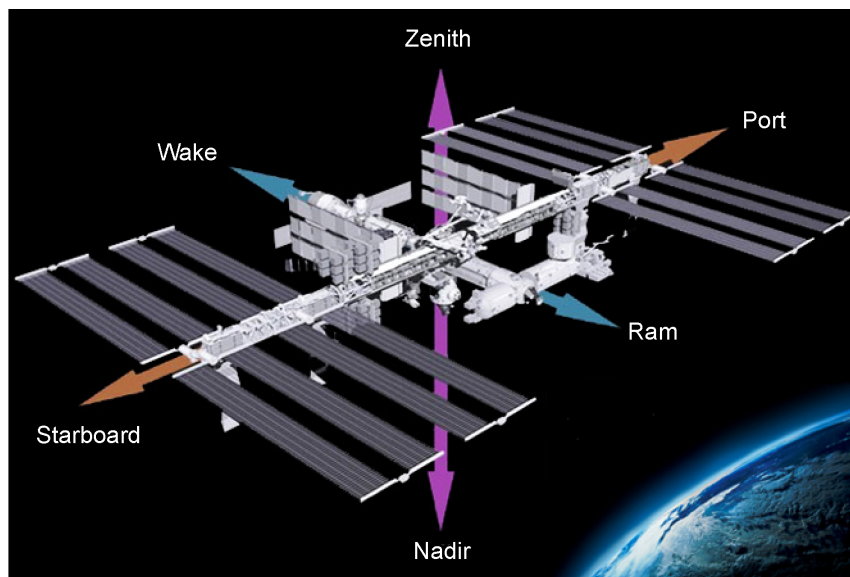

Figure 4.—Diagram showing ram (flight direction), wake, zenith, and nadir directions on the International Space Station.

Table 1 provides a summary of the MISSE 1–8 missions. There were six missions with a total of 10 PECs and one smaller tray called the Optical Reflector Materials Experiment III Ram/Wake (ORMatE-III R/W) that were flown along with 1000s of test samples.

Erosion Yield and Atomic Oxygen Fluence Determination

Mass-Based Erosion Yield

A common technique for determining the E_y of materials is based on mass loss of flight samples and is calculated using dehydrated mass measurements before and after flight. The E_y of the sample is determined through the following equation:

$$E_y = \frac{\Delta M_S}{\left(A_S \rho_S F\right)}$$

(1)

where

E_y = erosion yield of flight sample (cm³/atom)
ΔM_S = mass loss of the flight sample (g)
A_S = surface area of the flight sample exposed to AO (cm²)
ρ_S = density of flight sample (g/cm³)
F = low Earth orbit AO fluence (atoms/cm²)

Table 1. MISSE 1–8 Mission and Space Exposure Summary

MISSE PEC	Launch Mission	Date Placed Outside ISS	Location on ISS	Tray Orientation	Retrieval Mission	Date Retrieved from Outside of ISS	LEO Exposure Duration (years)
1 and 2	STS-105	8/16/2001	PEC 1: High Pressure Gas Tank (HPGT) PEC 2: Quest Airlock	Ram and Wake	STS-114	7/30/2005	3.95
3 and 4	STS-121	8/3/2006*	PEC 3: HPGT PEC 4: Quest Airlock	Ram and Wake	STS-118	8/18/2007	1.04
5	STS-114	8/3/2005	Aft P6 Trunion Pin Handrail	Zenith and Nadir	STS-115	9/15/2006	1.12
6A and 6B	STS-123	3/22/2008	Columbus Laboratory	Ram and Wake	STS-128	9/1/2009	1.45
7A and 7B	STS-129	11/23/2009	EXPRESS Logistics Carrier 2 (ELC 2) on S3 Truss	7A: Zenith and Nadir 7B: Ram and Wake	STS-134	5/20/2011	1.49
8 and ORMatE-III R/W†	STS-134 STS-135#	8: 5/20/2011 ORMatE-III R/W: 7/12/2011#	EXPRESS Logistics Carrier 2 (ELC 2) on S3 Truss	8: Zenith and Nadir ORMatE-III R/W: Ram and Wake	SpaceX-3 Dragon	7/9/2013	MISSE 8: 2.14 ORMatE-III: 2.00

*Deployed during Expedition 13.
†ORMatE-III R/W: Optical Reflector Materials Experiment III Ram/Wake.
#ORMatE III deployment EVA occurred 7/12/11 during the STS-135 mission.

Atomic Oxygen Fluence Determination

The AO fluence (F) of a spaceflight mission can be determined through the mass loss of a Kapton® H witness sample because Kapton® H has a well characterized erosion yield, E_K (3.0×10^{-24} cm³/atom) in the LEO environment.[11–14] Therefore, the AO fluence can be calculated using the following equation:

$$F = \frac{\Delta M_K}{\left(A_K \rho_K E_K \right)} \tag{2}$$

where

F = low Earth orbit AO fluence (atoms/cm²)
ΔM_K = mass loss of Kapton® H witness sample (g)
A_K = surface area of Kapton® H witness sample exposed to AO (cm²)
ρ_K = density of Kapton® H witness sample (1.4273 g/cm³)[18]
E_K = erosion yield of Kapton® H witness sample (3.0×10^{-24} cm³/atom)

Recession-Depth-Based Erosion Yield

Recession measurements can also be used for AO E_y determination based on erosion depth step-heights. The erosion or recession depth (D) can be measured from a protected surface using profilometry, scanning electron microscopy (SEM), optical interferometry, or atomic force microscopy for low-fluence exposures.[25] The recession based E_y can be calculated through the following equation:

$$E_y = \frac{D}{F} \tag{3}$$

where

E_y = erosion yield of flight sample (cm³/atom)
D = erosion depth of flight sample (cm)
F = low Earth orbit AO fluence (atoms/cm²)

The recession depth technique used for some of the Glenn MISSE flight samples involved pre-flight protection of the sample surface using isolated small salt (NaCl) particles that are in intimate contact with the sample.[25,26] The salt particles are applied to the sample substrate by spraying a saturated salt solution using an atomizer. This results in isolated, protective particles that typically remain in contact on the surface during flight and retrieval. The particles are then removed post-flight by washing off the salt with distilled water followed by drying with nitrogen gas.[25,26] The recession depth was then determined using SEM.

Using SEM, images were obtained at a 40° tilt angle and D was determined using the following equation:

$$D = \frac{d}{\sin \theta} \tag{4}$$

where

D = erosion depth of flight sample (cm)
d = erosion depth measured from SEM image obtained at θ tile angle (cm)
θ = SEM tilt angle (degrees)

The SEM-image-based erosion depth (d) was measured from the top of the protected surface to the mid-length of the remaining erosion cones.

Experiment Procedures

Mass Loss

One of the critical issues with using mass loss for obtaining accurate E_y data is that dehydrated mass measurements are needed. Many polymer materials, such as Kapton®, are very hygroscopic (absorbing up to 2 percent of their weight in moisture) and can fluctuate in mass with humidity and temperature. Therefore, for accurate mass loss measurements to be obtained, it is necessary that the samples be fully dehydrated (i.e., in a vacuum desiccator) immediately prior to measuring the mass both pre-flight and post-flight.

MISSE flight samples were dehydrated in a vacuum desiccator maintained at a pressure of 8.0 to 13.3 Pa (60 to 100 mtorr) with a mechanical roughing pump. Typically, five flight samples and their corresponding control samples were placed in a vacuum desiccator, in a particular order, and left under vacuum for a minimum of 72 hours. Once a sample was removed for weighing, the vacuum desiccator was immediately put back under vacuum to keep the other samples under vacuum. Previous tests showed that the mass of a dehydrated sample was not adversely affected if the desiccator was opened and quickly closed again and pumped back down to approximately 20 Pa (150 mtorr) prior to that sample being weighed. This process allows multiple samples to be dehydrated together. The time at which the sample was first exposed to air was recorded along with the times at which it was weighed. A total of three mass readings were obtained and averaged. The total time it took to obtain the three readings, starting from the time air was let into the desiccator, was typically 5 minutes. The samples were weighed pre-flight using a Sartorius ME 5 Microbalance (0.000001 g sensitivity). Heavier samples, such as PG were measured using a Sartorius Balance R160P (0.00001 g sensitivity). Records of the following were kept: the sequence of sample weighing, the number of samples in each set, the time under vacuum prior to weighing, the temperature and humidity in the room, the time air was let into the desiccator, and the time a sample was taken out of the desiccator, the time of each weighing and the mass. The same procedure and sequence was repeated with the same samples post-flight.

Density

The densities of the majority of samples were based on density gradient column measurements of polymers made for the MISSE 2 Polymers experiment.[2,18] The density gradient columns were created in 50-mL burets either with solvents of cesium chloride (CsCl, density $\rho \approx 2$ g/cm^3) and water (H$_2$O, $\rho =$ 1.0 g/cm^3) for less dense polymers such as Kapton® H or with solvents of carbon tetrachloride (CCl$_4$, $\rho = 1.594$ g/cm^3) and bromoform (CHBr$_3$, $\rho = 2.899$ g/cm^3) for more dense polymers such as the fluoropolymers. A quadratic calibration curve was developed for each column based on the equilibrium vertical position of three to four standards of known density (± 0.0001 g/cm^3). Subsequently, density values of samples were calculated based on the vertical positions of small (<2 mm) pieces placed into the column and allowed to settle for 2 hours. Where possible, the same batch of material was used for all the Glenn MISSE polymers experiments. The manufacturers' densities were used for several polymers, as noted in the experiment papers.

Surface Area Measurements

Typically, the exposed sample area was determined by measuring the diameter of the flight sample tray opening using digital calipers. For the 1-in. circular trays, such as those for the MISSE 2 experiment, each specific tray opening was measured at 10 different diameter orientations to determine an average diameter. This diameter was then used to compute the sample area exposed to LEO AO for each sample position. For the MISSE 8 flight sample trays, the exposed surface areas of the ram, wake, and zenith tray samples were determined by averaging four different diameter measurements of each sample tray opening obtained with a bore gauge (± 0.001 mm). The exposed surface area of the taped samples was determined using AutoCAD® (Autodesk, Inc.) computer design software to trace the exposed border of the sample on

a sample photograph. The sample photograph was taken, along with a scale bar, with a Sony DSC-T7 digital camera on a Polaroid Land camera stand. The surface area was computed using AutoCAD® based on the traced area as well as measurements of the scale bar.

MISSE 2–8 Polymer Experiments

As previously mentioned, the data provided is a compiled list of E_y values for the ram samples from six Glenn experiments flown on MISSE PECs 2, 4, 6, 7, and 8. Table 2 provides a list of the Glenn experiment titles along with the MISSE mission, MISSE PEC, AO fluence, and solar exposure for the ram samples and provides reference information for the flight data. As stated previously, although these are primarily polymer experiments, other materials such as PG, composites, and protective coatings were included as part of the experiments. Figures 5 to 9 provide on-orbit images of the MISSE missions. More details on the individual experiments can be found in references listed in Table 2. A list of the samples flown as part of the Glenn MISSE 2–8 polymers experiments is provided in Table 3.

Table 2. NASA Glenn Research Center MISSE 2–8 Ram Exposure Experiments

Glenn Experiment	MISSE Mission	MISSE PEC	Ram AO Fluence, atoms/cm²	Ram Solar Exposure, ESH	Number of Ram E_y Samples (AO F[a])	Reference
Polymers Erosion and Contamination Experiment (PEACE) Polymers Experiment	1 and 2	2	8.43×10^{21}	6,300	41 (2)	2, 18
Polymer Film Thermal Control (PFTC) and Gossamer Materials Experiments			8.51×10^{21}	~5300 to ~6200	4	27
Polymer Film Thermal Control (PFTC) and Gossamer Materials Experiments	3 and 4	4	2.15×10^{21}	1,200 to 1,600	7 (1)	28
Stressed Polymers Experiment	6A and 6B	6A	1.97×10^{21}	2,600	24 (2)	19
Polymers Experiment	7A and 7B	7B	4.22×10^{21}	2,400	30 (1)	20, 21, 29
Polymers Experiment	8	ORMatE-III R/W	4.62×10^{21}	~3,200	7 (1)	22

[a]Includes Kapton® H samples for AO F (fluence) determination.

Figure 5.—Astronaut Patrick Forrester installs MISSE PEC 2 on the ISS Quest Airlock during a spacewalk on August 16, 2001.

Figure 6.—MISSE PEC 4 ram tray during Expedition 15 mission in July 2007.
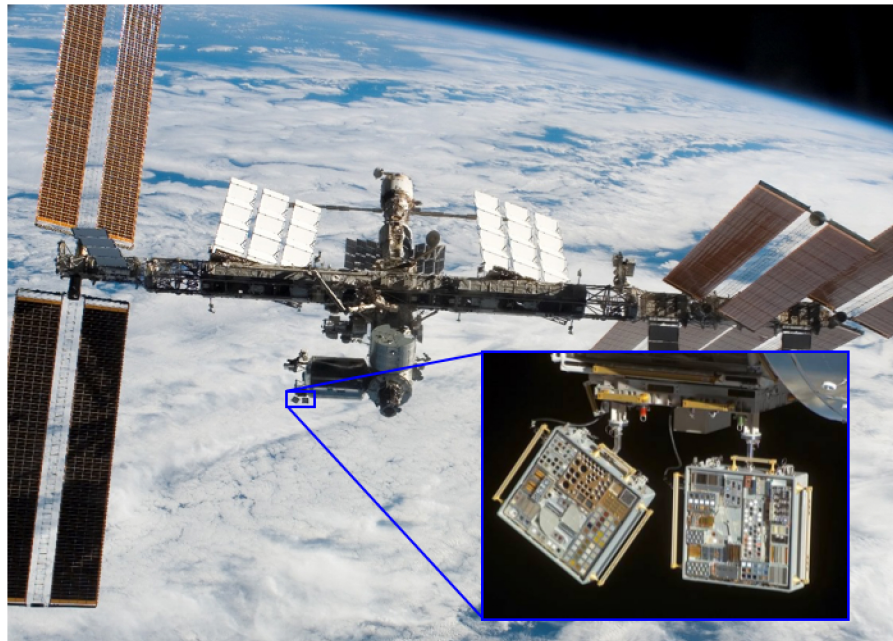
Figure 7.—International Space Station (photographed in March 2008) with close-up of MISSE 6A and 6B on the Columbus Laboratory.
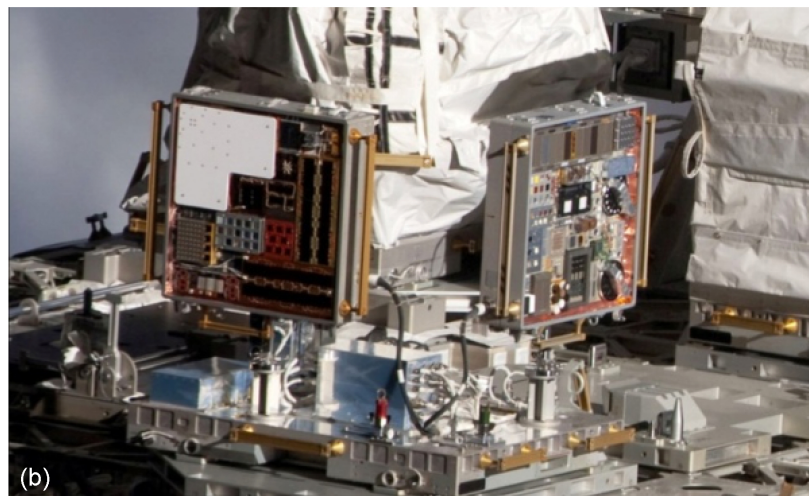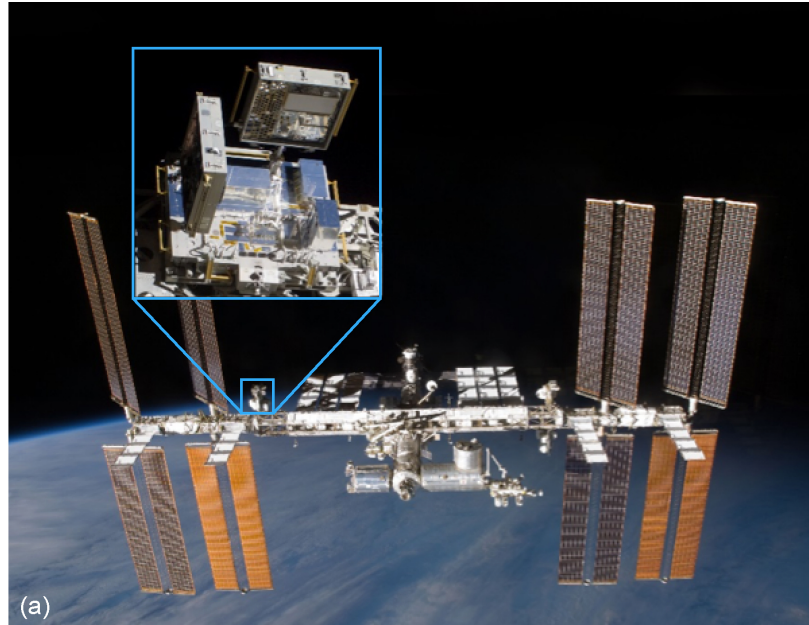
Figure 8.—MISSE 7A and 7B on the ISS EXPRESS Logistics Carrier 2 (ELC-2). (a) Location of MISSEs 7A and 7B on the ISS ELC-2 as imaged during STS-129 shuttle mission in November 2009 shortly after deployment. (b) On-orbit photograph of MISSE 7A (left, zenith surface shown) and 7B (right, ram surface shown) as imaged on-orbit during the STS-130 shuttle mission in February 2010.
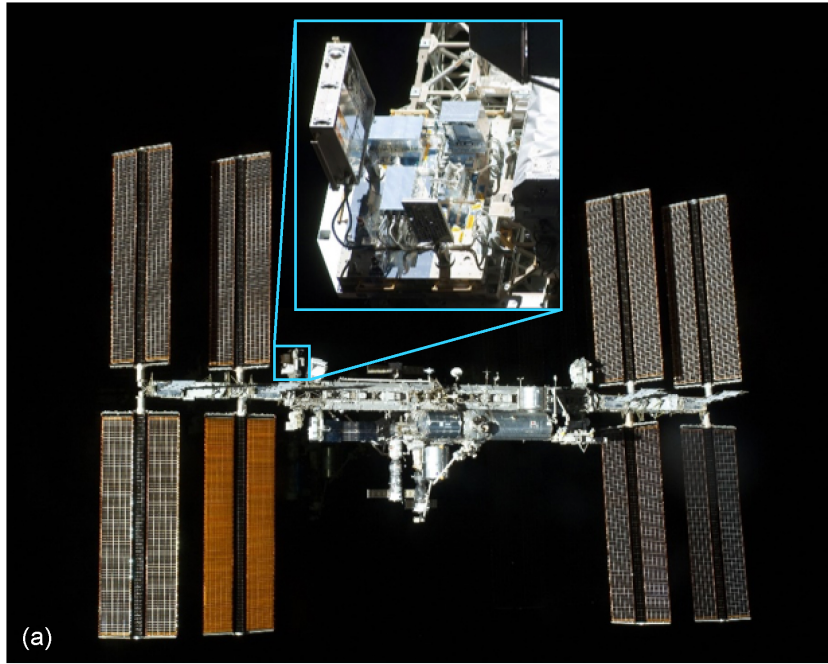
Figure 9.—MISSE 8 PEC and ORMatE-III on the ISS ELC-2. (a) During the
STS-135 shuttle mission in July 2011 shortly after deployment of ORMatE-III.
(b) On-orbit image of the ram surface of ORMatE-III in July 2013.

MISSE 2–8 Ram Erosion Data

The MISSE 2–8 ram E_y values are provided in Table 3. A total of 71 types of materials with 111 E_y values are provided. Seven Kapton® H flight samples, used to determine the mission AO fluence based on a previously characterized LEO E_y (3.0×10^{-24} cm³/atom), are included. Therefore, 104 new E_y values were determined as part of the Glenn MISSE 2–8 polymer flight experiments. Often the same material was flown on different missions so that trends for E_y versus AO fluence and/or solar exposure could be determined. These "repeat" samples include Teflon™ FEP, PTFE, white Tedlar® (E. I. du Pont de Nemours and Company), high-temperature polyimide (PMR-15), clear polyimide (CP1™), Upilex®-S (UBE Europe GmbH)), Kapton® HN, Mylar® (E. I. du Pont de Nemours and Company), and polybenzimidazole (PBI).

The E_y values for uncoated polymers range from 3.81×10^{-27} cm³/atom for DC 93–500 silicone exposed to an AO fluence of 4.62×10^{21} atoms/cm² on MISSE 8 to 9.14×10^{-24} cm³/atom for polyoxymethylene (POM) exposed to an AO fluence of 8.43×10^{21} atoms/cm² on MISSE 2. The E_y for the DC 93–500 silicone, 3.81×10^{-27} cm³/atom, is 3 orders of magnitude lower than that for Kapton® H, as indicated by the extremely low mass loss (0.076 mg). As mentioned previously, silicones convert to a glassy silicate layer with AO exposure. Unfortunately, the silicate layer typically contains many mud-tile-like cracks, which continue to develop with further AO exposure.[30] One polymer, Triton oxygen resistant, low omdulus (TOR™ LM; Triton Systems, Inc.), experienced mass gain when exposed to an AO fluence of 2.15×10^{21} atoms/cm² on MISSE 4. Although it appears to be durable to AO, TOR™ LM becomes brittle with space exposure. As one example, Miller and Dever found that a MISSE 5 TOR™ LM sample lost 49 percent of its percent elongation after 13 months of nadir space exposure.[31]

The prediction of E_y based on computational modeling and/or ground laboratory testing has been performed using many of the polymers listed in Table 3. Computational modeling was used to simulate the LEO E_y of 38 polymers and PG by utilizing information on the chemical structure and measured physical properties of the polymers.[32] The resulting predictive tool results had a correlation coefficient of 0.895 when compared with actual MISSE 2 space E_y data. Modeling of E_y based on ground lab hyperthermal asher data for 26 polymers (excluding FEP and PTFE) was able to predict space E_y results within ±37.5 percent of MISSE 2 results and were a factor of ~4 more accurate than thermal energy asher predictions.[33]

Table 3. Atomic Oxygen (AO) Erosion Yields E_y From MISSE 2–8 Ram Polymer Experiments

Material [trade names][a]	Sample abbreviation	Thickness, mil	MISSE 2 ram AO = 8.43×10²¹ atom/cm² Solar = 6,300 ESH Mission: 4 years (Ref. 18)		MISSE 4 ram AO = 2.15×10²¹ atom/cm² Solar = 1,400 ESH Mission: 1 year (Ref. 28)		MISSE 6B ram (nonstressed) AO = 1.97×10²¹ atom/cm² Solar = 2,600 ESH Mission: 1.5 years (Ref. 19)		MISSE 7B ram AO = 4.22×10²¹ atom/cm² Solar = 2,400 ESH Mission: 1.5 years (Ref. 21)		MISSE 8 ram AO = 4.62×10²¹ atom/cm² Solar ≈ 3,200 ESH Mission: 2 years (Ref. 22)	
			ID (layers) (Ref. 2)	AO E_y, cm³/atom	ID (layers)	AO E_y, cm³/atom	ID (layers)	AO E_y, cm³/atom	ID[b] (layers)	AO E_y, cm³/atom	ID (layers)	AO E_y, cm³/atom
Acrylonitrile butadiene styrene [Cycolac™, Absylux®]	ABS	5	2-E5-6 (3)	1.09×10⁻²⁴								
Allyl diglycol carbonate [CR-39®, Homalite H-911]	ADC	31, 47	2-E5-14 (1)	[c]>6.80×10⁻²⁴			W3-6/N14-S (1)	8.28×10⁻²⁴				
Amorphous fluoropolymer [Teflon® AF 1601]	AF	2	2-E5-45 (1)	1.98×10⁻²⁵								
Cellulose acetate [Clarifoil, Tenite™ Acetate; Dexel]	CA	2	2-E5-7 (13)	5.05×10⁻²⁴								
Cellulose nitrate; nitrocellulose membrane	CN	5							N5-14 (7)	[c]>6.58×10⁻²⁴		
Chlorotrifluoroethylene [Kel-F, Neoflon® M-300]	CTFE	5	2-E5-39 (1)	8.31×10⁻²⁵								
Carbon: diamond, single crystal natural Class IIA, 100 plane	Diamond	10							B7-6 (1)	1.58±0.40×10⁻²⁶ (Ref. 29)		
Carbon: highly oriented pyrolytic graphite, basal plane	HOPG-BP	58							B7-6	1.05±0.08×10⁻²⁴ (Ref. 29)		
Carbon: highly oriented pyrolytic graphite, edge (a,b) plane	HOPG-EP	58							B7-6	5.38±0.90×10⁻²⁵ (Ref. 29)		
Carbon: pyrolytic graphite, C plane	PG	80	2-E5-25 (1)	4.15×10⁻²⁵								
Copolymer of polytetrafluoroethylene, perfluoropropyl vinyl ether, and perfluoromethyl vinyl ether [Hyflon® MFA® 620]	MFA	4							M7BT-E15 (1)[d]	1.07×10⁻²⁵		
Crystalline polyvinyl fluoride with white pigment [White Tedlar®]	PVF-W	2							B7-1 (1)	1.48×10⁻²⁵		
Crystalline polyvinyl fluoride with white pigment and a 0.5-mil Kapton® H cover [White Tedlar®]	PVF-W	2							B7-2 (1) AO fluence = 3.79×10²¹	1.54×10⁻²⁵		
Crystalline polyvinyl fluoride with white pigment and two 0.5-mil Kapton® H covers [White Tedlar®]	PVF-W	2							B7-3 (1): AO fluence = 3.37×10²¹	1.67×10⁻²⁵		
Crystalline polyvinyl fluoride with white pigment [White Tedlar® TW10B53]	PVF-W	1	2-E5-11 (13)	1.01×10⁻²⁵							M8-R5 (7)	1.45×10⁻²⁵

Table 3. Atomic Oxygen (AO) Erosion Yields E_y From MISSE 2–8 Ram Polymer Experiments

Material [trade names][a]	Sample abbreviation	Thickness, mil	MISSE 2 ram AO = 8.43×10²¹ atom/cm² Solar = 6,300 ESH Mission: 4 years (Ref. 18)		MISSE 4 ram AO = 2.15×10²¹ atom/cm² Solar = 1,400 ESH Mission: 1 year (Ref. 28)		MISSE 6B ram (nonstressed) AO = 1.97×10²¹ atom/cm² Solar = 2,600 ESH Mission: 1.5 years (Ref. 19)		MISSE 7B ram AO = 4.22×10²¹ atom/cm² Solar = 2,400 ESH Mission: 1.5 years (Ref. 21)		MISSE 8 ram AO = 4.62×10²¹ atom/cm² Solar ≈ 3,200 ESH Mission: 2 years (Ref. 22)	
			ID (layers) (Ref. 2)	AO E_y, cm³/atom	ID (layers)	AO E_y, cm³/atom	ID (layers)	AO E_y, cm³/atom	ID[b] (layers)	AO E_y, cm³/atom	ID (layers)	AO E_y, cm³/atom
Cyanate ester composite [FG-120 fiber glass/EX-1515 cyanate ester]	CE	39							M7BT-E19 (1)[d]	2.41×10⁻²⁵		
Cyanate ester composite [Torayca® M55J carbon fiber/954-3 cyanate ester]	CE	35							M7BT-E20 (1)[d]	5.38×10⁻²⁵		
Cyanate siloxane composite [Torayca® M55J carbon fiber/996 cyanate siloxane]	CE Si	35							M7BT-E21 (1)[d]	3.44×10⁻²⁵		
Epoxide; epoxy [Hysol® EA 956]	EP	88 to 92	2-E5-19 (1)	4.21×10⁻²⁴								
Ethylene chlorotrifluoroethylene [Halar® 300]	ECTFE	3	2-E5-40 (3)	1.79×10⁻²⁴								
Ethylene tetrafluoroethylene [Tefzel® ZM]	ETFE	3	2-E5-41 (2)	9.61×10⁻²⁵								
Fluorinated ethylene propylene [Teflon® FEP]	FEP	2	2-E5-42 (1)	2.00×10⁻²⁵							M9-R9 (1)	2.37×10⁻²⁵
Fluorinated ethylene propylene [Teflon® FEP]	FEP	5					W2-10/ N2 (4)	1.69×10⁻²⁵				
Fluorinated ethylene propylene, back-surface aluminized [aluminized Teflon® FEP]	FEP/Al	5	2-E6-13 (1)[e]	2.11×10⁻²⁵			W6-6 (1)[f]	2.28×10⁻²⁵	N5-4 (1)	1.81×10⁻²⁵	M8-R2 (1)	2.39×10⁻²⁵
Fluorinated ethylene propylene, back-surface carbon-painted [carbon-painted Teflon® FEP]	FEP/C	2							M7BT-E16 (1)[d]	1.57×10⁻²⁵		
Fluorinated ethylene propylene/Al, preflight heated 380 hr at 200 °C	Heated FEP/Al	5					W6-11 (1)[f]	2.26×10⁻²⁵				
Fluorinated ethylene propylene/Ag/Inconel, flown on LDEF, Ag-FEP F-04, 10,458 ESH	LDEF Ag-FEP	5					W6-13 (1)[f]	2.37×10⁻²⁵				
Hubble Space Telescope fluorinated ethylene propylene/Al, 1st servicing mission, SM1 MSS-D: 3.6 yr, 11,339 ESH	HST FEP/Al	5					W6-8 (1)[f]	2.40×10⁻²⁵				
Hubble Space Telescope fluorinated ethylene propylene/Al, 3rd servicing	HST FEP/Al	5					W6-7 (1)[f]	2.11×10⁻²⁵			M8-R6 (1)	2.50×10⁻²⁵

Table 3. Atomic Oxygen (AO) Erosion Yields E_y From MISSE 2–8 Ram Polymer Experiments

Material [trade names][a]	Sample abbreviation	Thickness, mil	MISSE 2 ram AO = 8.43×10^{21} atom/cm² Solar = 6,300 ESH Mission: 4 years (Ref. 18)		MISSE 4 ram AO = 2.15×10^{21} atom/cm² Solar = 1,400 ESH Mission: 1 year (Ref. 28)		MISSE 6B ram (nonstressed) AO = 1.97×10^{21} atom/cm² Solar = 2,600 ESH Mission: 1.5 years (Ref. 19)		MISSE 7B ram AO = 4.22×10^{21} atom/cm² Solar = 2,400 ESH Mission: 1.5 years (Ref. 21)		MISSE 8 ram AO = 4.62×10^{21} atom/cm² Solar ≈ 3,200 ESH Mission: 2 years (Ref. 22)	
			ID (layers) (Ref. 2)	AO E_y, cm³/atom	ID (layers)	AO E_y, cm³/atom	ID (layers)	AO E_y, cm³/atom	ID[b] (layers)	AO E_y, cm³/atom	ID (layers)	AO E_y, cm³/atom
mission, SM3A R1: 9.7 yr, 13,598 ESH												
Hubble Space Telescope fluorinated ethylene propylene/Al, 3rd servicing mission, SM3A R5: 9.7 yr, >30,321 ESH	HST FEP/Al	5					W6-12 (1)[f]	2.34×10^{-25}				
Fluorinated ethylene propylene, TiO₂/Al₂O₃ coated	TiO₂/Al₂O₃/FEP	2							B7-11 (1)	7.99×10^{-28}		
Fluorinated ethylene propylene, back-surface vapor-deposited silver/niobium coated	FEP/VDS/Nb	5			2-E22-29 (1)	1.28×10^{-25}						
Germanium-coated (25 Å) Kapton® XC with Nomex® scrim	Ge/KaptonXC/ Scrim	1			2-E22-16 (1)	1.65×10^{-26}						
High-temperature polyimide resin [PMR-15]	PI (PMR-15)	13	2-E5-34 (1)	[c]$>3.02\times10^{-24}$								
High-temperature polyimide resin [PMR-15]	PI (PMR-15)	34					W2-7/ N12 (1)	[g]2.68×10^{-24}				
Perfluoroalkoxy copolymer resin [Teflon® PFA 200 CLP]	PFA	2	2-E5-44 (4)	1.73×10^{-25}								
Poly(p-phenylene terephthalamide) [Kevlar® 29 fabric]	PPD-T	2.2	2-E5-8 (3)	6.28×10^{-25}								
Poly(p-phenylene-2,6-benzobis-oxazole) [Zylon®, balanced biaxial]	PBO	1	2-E5-18 (11)	1.36×10^{-24}								
Polyacrylonitrile [Barex® 210]	PAN	2	2-E5-13 (9)	1.41×10^{-24}								
Polyamide 6 [Nylon 6]	PA 6	2	2-E5-27 (8)	3.51×10^{-24}								
Polyamide 66 [Nylon 66]	PA 66	2	2-E5-28 (7)	1.80×10^{-24}								
Polyamide-imide [Torlon® 4203]	PAI	29							N5-12 (1)	1.74×10^{-24}		
Polybenzimidazole [Celazole® PBI 22]	PBI	2	2-E5-35 (4)	[c]$>2.21\times10^{-24}$								
Polybenzimidazole	PBI	4					W3-7/N12-S (5)	4.55×10^{-24}				
Polybutylene terephthalate [VALOX® 357]	PBT	1	2-E5-21 (5)	9.11×10^{-25}								

Table 3. Atomic Oxygen (AO) Erosion Yields E_y From MISSE 2–8 Ram Polymer Experiments

Material [trade names][a]	Sample abbreviation	Thickness, mil	MISSE 2 ram AO = 8.43×10^{21} atom/cm^2 Solar = 6,300 ESH Mission: 4 years (Ref. 18)		MISSE 4 ram AO = 2.15×10^{21} atom/cm^2 Solar = 1,400 ESH Mission: 1 year (Ref. 28)		MISSE 6B ram (nonstressed) AO = 1.97×10^{21} atom/cm^2 Solar = 2,600 ESH Mission: 1.5 years (Ref. 19)		MISSE 7B ram AO = 4.22×10^{21} atom/cm^2 Solar = 2,400 ESH Mission: 1.5 years (Ref. 21)		MISSE 8 ram AO = 4.62×10^{21} atom/cm^2 Solar ≈ 3,200 ESH Mission: 2 years (Ref. 22)	
			ID (layers) (Ref. 2)	AO E_y, cm^3/atom	ID (layers)	AO E_y, cm^3/atom	ID (layers)	AO E_y, cm^3/atom	ID[b] (layers)	AO E_y, cm^3/atom	ID (layers)	AO E_y, cm^3/atom
Polycarbonate [PEEREX® 61]	PC	10	2-E5-36 (2)	4.29×10^{-24}								
Polyetheretherketone [Victrex™ PEEK 450]	PEEK	3	2-E5-37 (6)	2.99×10^{-24}								
Polyetherimide [Ultem™ 1000)]	PEI	10	2-E5-26 (2)	[c]$>3.31\times10^{-24}$			W2-12/N13 (2)	3.37×10^{-24}				
Polyethersulfone	PES	3							N5-3 (6)	2.79×10^{-24}		
Polyethylene	PE	2	2-E5-9 (6)	[c]$>3.74\times10^{-24}$			W2-2/N10 (10)	4.05×10^{-24}	N5-1 (18)	4.11×10^{-24}		
Polyethylene oxide [Alkox® E-30 powder]	PEO	29	2-E5-17 (1)	1.93×10^{-24}					M7BT-E17 (1)[d]	2.75×10^{-24}		
Polyethylene terephthalate [Mylar® A-200]	PET	2	2-E5-38 (8)	3.01×10^{-24}								
Polyethylene terephthalate [Mylar® A-500]	PET	5					W2-13/N9 (4)	3.22×10^{-24}				
Polyimide, clear [CP1-300]	CP1	3	2-E5-29 (4)	1.91×10^{-24}								
Polyimide, clear [CP1]	CP1	1	2-E6-15 (9)[e]	1.91×10^{-24}	2-E22-26 (20)	2.26×10^{-24}	W2-4/N4 (20)	2.16×10^{-24}				
Polyimide, AO resistant [CORIN®]	CORIN	2							N5-15 (4)	3.05×10^{-26}		
Polyimide (BPDA) [Upilex®-S]	PI (Upilex-S)	1	2-E5-32 (11)	9.22×10^{-25}	2-E22-19 (21)	1.71×10^{-24}	W2-15/N3 (20)	1.65×10^{-24}				
Polyimide (BPDA) [Upilex®-S]	PI (Upilex-S)	1	2-E6-14 (9)[e]	9.76×10^{-25}								
Polyimide (PMDA) [Kapton® CB]	PI (Kapton CB)	5					W2-9/N5 (4)	2.70×10^{-24}				
Polyimide (PMDA) [Kapton® E]	PI (Kapton E)	2					W2-8/N7 (10)	2.83×10^{-24}				
Polyimide (PMDA) [Kapton® H]	Kapton H	5	2-E5-30 (3), 2-E5-33 (3)	[h]3.00×10^{-24}	2-E22-18 (7)	[h]3.00×10^{-24}	W2-3/N8 (4), W6-5/GW-1 (3)	[h]3.00×10^{-24}	B7-8 (4)	[h]3.00×10^{-24}	M8-R1 (4)	[h]3.00×10^{-24}
Polyimide (PMDA), 0.75-in. square [Kapton® H]	PI (Kapton H)	5							N5-5 (4)	3.05×10^{-24}		

Table 3. Atomic Oxygen (AO) Erosion Yields E_y From MISSE 2–8 Ram Polymer Experiments

Material [trade names][a]	Sample abbreviation	Thickness, mil	MISSE 2 ram AO = 8.43×10^{21} atom/cm² Solar = 6,300 ESH Mission: 4 years (Ref. 18) ID (layers) (Ref. 2)	AO E_y, cm³/atom	MISSE 4 ram AO = 2.15×10^{21} atom/cm² Solar = 1,400 ESH Mission: 1 year (Ref. 28) ID (layers)	AO E_y, cm³/atom	MISSE 6B ram (nonstressed) AO = 1.97×10^{21} atom/cm² Solar = 2,600 ESH Mission: 1.5 years (Ref. 19) ID (layers)	AO E_y, cm³/atom	MISSE 7B ram AO = 4.22×10^{21} atom/cm² Solar = 2,400 ESH Mission: 1.5 years (Ref. 21) ID[b] (layers)	AO E_y, cm³/atom	MISSE 8 ram AO = 4.62×10^{21} atom/cm² Solar ≈ 3,200 ESH Mission: 2 years (Ref. 22) ID (layers)	AO E_y, cm³/atom
Polyimide (PMDA), 10 layers 0.5-mil Kapton® H, with spacers, over two 5-mil layers Kapton® H	PI (Kapton H)	0.5					W6-9/ GW-3 (10)	3.25×10^{-24}				
Polyimide (PMDA), 10 layers 0.5-mil Kapton® H, no spacers, over one 5-mil Kapton® H layer	PI (Kapton H)	0.5					W6-10/ GW-2 (10)	3.08×10^{-24}				
Polyimide (PMDA) [Kapton® HN]	PI (Kapton HN)	5	2-E5-31 (3)	2.81×10^{-24}	2-E22-17 (7)	2.83×10^{-24}			N5-6 (4): AO fluence = 4.22×10^{-21}	3.01×10^{-24}		
PI (PMDA) [Kapton® HN]	PI (Kapton HN)	5	2-E6-16 (3)[e]	2.75×10^{-24}								
PI (PMDA), Kapton® HN with 0.5-mil Kapton® H cover	PI (Kapton HN)	5							N5-7 (4): AO fluence = 3.79×10^{-21}	2.85×10^{-24}		
PI (PMDA), Kapton® HN with two 0.5-mil Kapton® H covers	PI (Kapton HN)	5							N5-8 (4): AO fluence = 3.37×10^{-21}	2.20×10^{-24}		
Polyimide [Kapton® XC (10^{-7} ohm/sq)]	Kapton XC	5					W2-14/N6 (4)	2.20×10^{-24}				
Polyimide [Vespel®]	PI Vespel	20							B7-9 (1)	2.94×10^{-24}		
Polymethyl methacrylate, impact modified [Plexiglas®; Acrylite®]	PMMA	2	2-E5-16 (10)	[c]>5.60×10^{-24}			W3-11/ N15-S (10)	5.28×10^{-24}				
Polymethylpentene [TPX® DX845 Natural]	PMP	2							N5-2 (9)	4.45×10^{-24}		
Polyoxymethylene; acetal; polyformaldehyde [Delrin® acetal]	POM	10	2-E5-12 (5)	9.14×10^{-24}								
Polyphenylene isophthalate [Nomex® Crepe Paper T-410]	PPPA	2	2-E5-24 (6)	1.41×10^{-24}								
Polypropylene [Contour® 28]	PP	20	2-E5-20 (1)	2.68×10^{-24}					M7BT-E14 (1)[d]	3.12×10^{-24}		
Polystyrene [Trycite™ 1000]	PS	2	2-E5-15 (11)	3.74×10^{-24}								

Table 3. Atomic Oxygen (AO) Erosion Yields E_y From MISSE 2–8 Ram Polymer Experiments

Material [trade names][a]	Sample abbreviation	Thickness, mil	MISSE 2 ram AO = 8.43×10²¹ atom/cm² Solar = 6,300 ESH Mission: 4 years (Ref. 18)		MISSE 4 ram AO = 2.15×10²¹ atom/cm² Solar = 1,400 ESH Mission: 1 year (Ref. 28)		MISSE 6B ram (nonstressed) AO = 1.97×10²¹ atom/cm² Solar = 2,600 ESH Mission: 1.5 years (Ref. 19)		MISSE 7B ram AO = 4.22×10²¹ atom/cm² Solar = 2,400 ESH Mission: 1.5 years (Ref. 21)		MISSE 8 ram AO = 4.62×10²¹ atom/cm² Solar ≈ 3,200 ESH Mission: 2 years (Ref. 22)	
			ID (layers) (Ref. 2)	AO E_y, cm³/atom	ID (layers)	AO E_y, cm³/atom	ID (layers)	AO E_y, cm³/atom	ID[b] (layers)	AO E_y, cm³/atom	ID (layers)	AO E_y, cm³/atom
Polysulfone "[Thermalux® (Udel® P-1700 NT 11)]	PSU	2	2-E5-22 (6)	2.94×10⁻²⁴								
Polytetrafluoroethylene [CHEMFILM® DF100]	PTFE	2	2-E5-43 (1)	1.42×10⁻²⁵							M8-R7 (1)	1.94×10⁻²⁵
Polytetrafluoroethylene [CHEMFILM® DF100]	PTFE	5					W2-5/N1 (4)	1.33×10⁻²⁵				
Polyurethane [Dureflex® PS8010]	PU	2	2-E5-23 (9)	1.56×10⁻²⁴								
Polyvinyl alcohol [MonoSol M1000]	PVOH	1.5							N5-13 (24)	3.14×10⁻²⁴		
Polyvinyl chloride [Clear-Lay® rigid PVC]	PVC	5							B7-10 (1)	c>1.74×10⁻²⁴		
Polyvinylfluoride Tedlar® TTR10SG3)	PVF	1	2-E5-10 (13)	3.19×10⁻²⁴								
Polyvinylidene fluoride [Kynar® 740]	PVDF	3	2-E5-46 (2)	1.29×10⁻²⁴								
Silicone [DC 93-500 on fused silica]	DC 93-500	10									M8-R10 (1)	3.81×10⁻²⁷
Triton oxygen resistant, low modulus polymer[i] [TOR™ LM]	TOR	1.5			2-E22-30 (1)	Mass gain						
Urethane/Vectran™ mesh	Ur/Vectra	10							N5-16 (1)	4.61×10⁻²⁵		

[a] Trade name owners are listed in the appendix.

[b] MISSE 7 N5 samples were 0.75- by 0.75-in. square, and B7 samples were 1- by 1-in. square.

[c] E_y is greater than this value because the sample was fully or partially eroded through all layers.

[d] Taped in thin Al holder.

[e] AO fluence for this tray was determined to be 8.51×10²¹ atoms/cm² (Ref. 27).

[f] Not previously published data (not included in Ref. 19).

[g] Residue on the surface, may have impact E_y.

[h] Kapton® H was used to determine the mission AO fluence using LEO E_y from prior flight experiments (3.00×10⁻²⁴ cm³/atom).

[i] Based on the pol(arylene ether benzimidazoles) class of polymers.

Atomic Oxygen Erosion Morphologies

Examples of erosion texturing morphologies for various polymers, varying structural orientations and forms of PG, and diamond exposed to LEO ram AO are provided in Figures 10 to 17. Figures 10 to 12 provide different AO erosion cone structures for three different polymers from the MISSE 2 PEACE Polymers experiment. Figure 10 is a high-magnification image (obtained at 10,000×) showing the development of very small cones on back surface aluminized Teflon™ fluorinated ethylene propylene (Al-FEP). The Al-FEP had an E_y of 2.11×10^{-25} cm^3/atom.[27] Figure 11 is a lower magnification image (obtained at 1,000×) showing the development of larger cones on chlorotrifluoroethylene (CTFE). The MISSE 2 CTFE had an E_y of 8.31×10^{-25} cm^3/atom, which is 4× greater than the E_y for Al-FEP.[18] Figure 12 provides a lower magnification image (obtained at 1,000×) showing development of much larger, high-aspect-ratio cones on an eroded MISSE 2 Kapton® H sample. This is the second layer of a multilayer stacked sample (three 5-mil-thick layers). These cones have AO-durable ash residual on the tips, as can be seen in Figure 12. As stated previously, Kapton® H has an E_y of 3.00×10^{-24} cm^3/atom (3.6× greater than the E_y for CTFE). As can be seen in these examples, the cone size often correlates to the E_y, and hence the extent of erosion.

Class IIa diamond (100 plane) flown on MISSE 7 was found to erode with ram AO exposure, but it had an extremely low E_y of $1.58 \pm 0.40 \times 10^{-26}$ cm^3/atom, which is 300× less than Kapton® H.[29] Scanning electron microscope images of the AO erosion texture of the Class IIa diamond are provided in Figure 13. Figure 13(a), taken at 10,000× magnification, shows the AO erosion texture. Figure 13(b) is a very high magnification image (taken at 40,000×) showing "typical" ram AO erosion cones. Figure 13(c) is a 25,000× magnification image of a salt-protected (top) and AO-exposed (bottom) border. The ratio of texture height (A) to the actual erosion depth (D), A/D, for the MISSE 7 Class IIa diamond was determined to be 0.879.[29]

Pyrolytic graphite (PG) and highly oriented pyrolytic graphite (HOPG) basal and edge planes displayed significantly different AO erosion morphologies; particularly, the basal plane HOPG. The MISSE 2 ram exposure PG sample developed a velvet black appearance, as can be seen in Figure 14. The MISSE 2 PG had an E_y of $4.15 \pm 0.45 \times 10^{-25}$ cm^3/atom. Scanning electron miscopy images of the erosion texture are provided in Figure 15. As can be seen, the MISSE 2 PG, which was exposed to 4 years of AO ram exposure (AO fluence of 8.43×10^{21} atoms/cm^2), developed typical AO erosion cones. Once again, however, the cone size for PG is smaller than for Kapton® H, consistent with the smaller E_y (the PG E_y is 7.2× less than for Kapton® H).

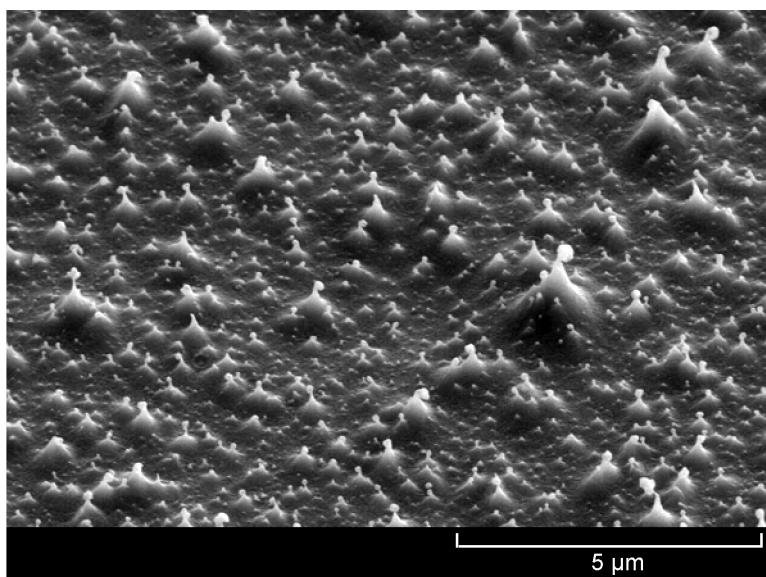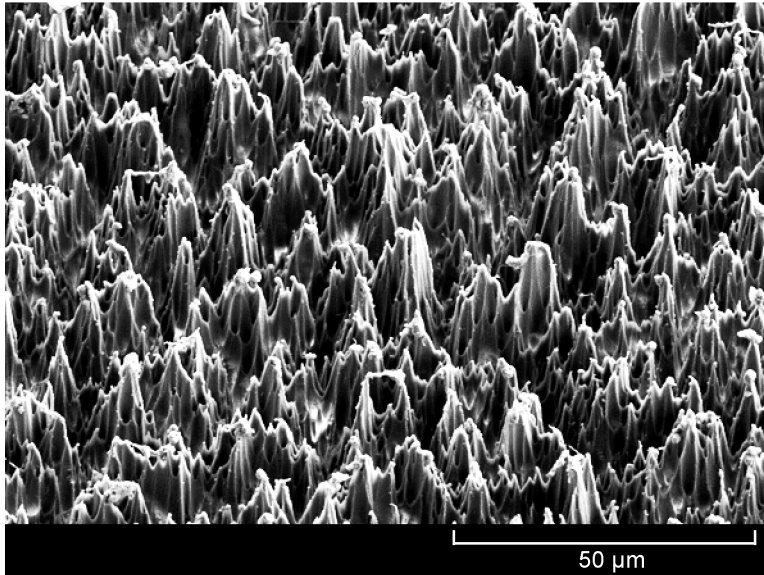Figure 10.—Erosion texture of MISSE 2 Al-FEP (10,000×, 45° tilt).[34]

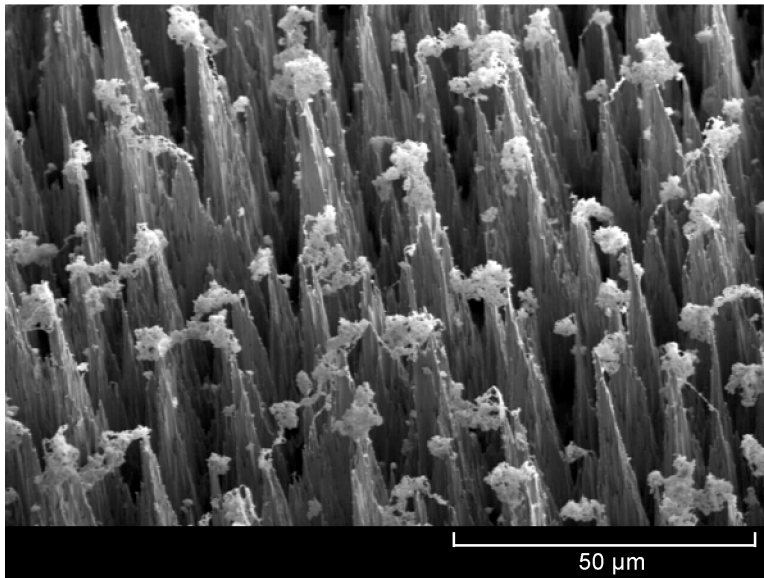Figure 11.—Erosion texture of MISSE 2 CTFE (1,000×, 45° tilt).[34]

Figure 12.—Erosion texture of MISSE 2 Kapton® H showing high aspect ratio
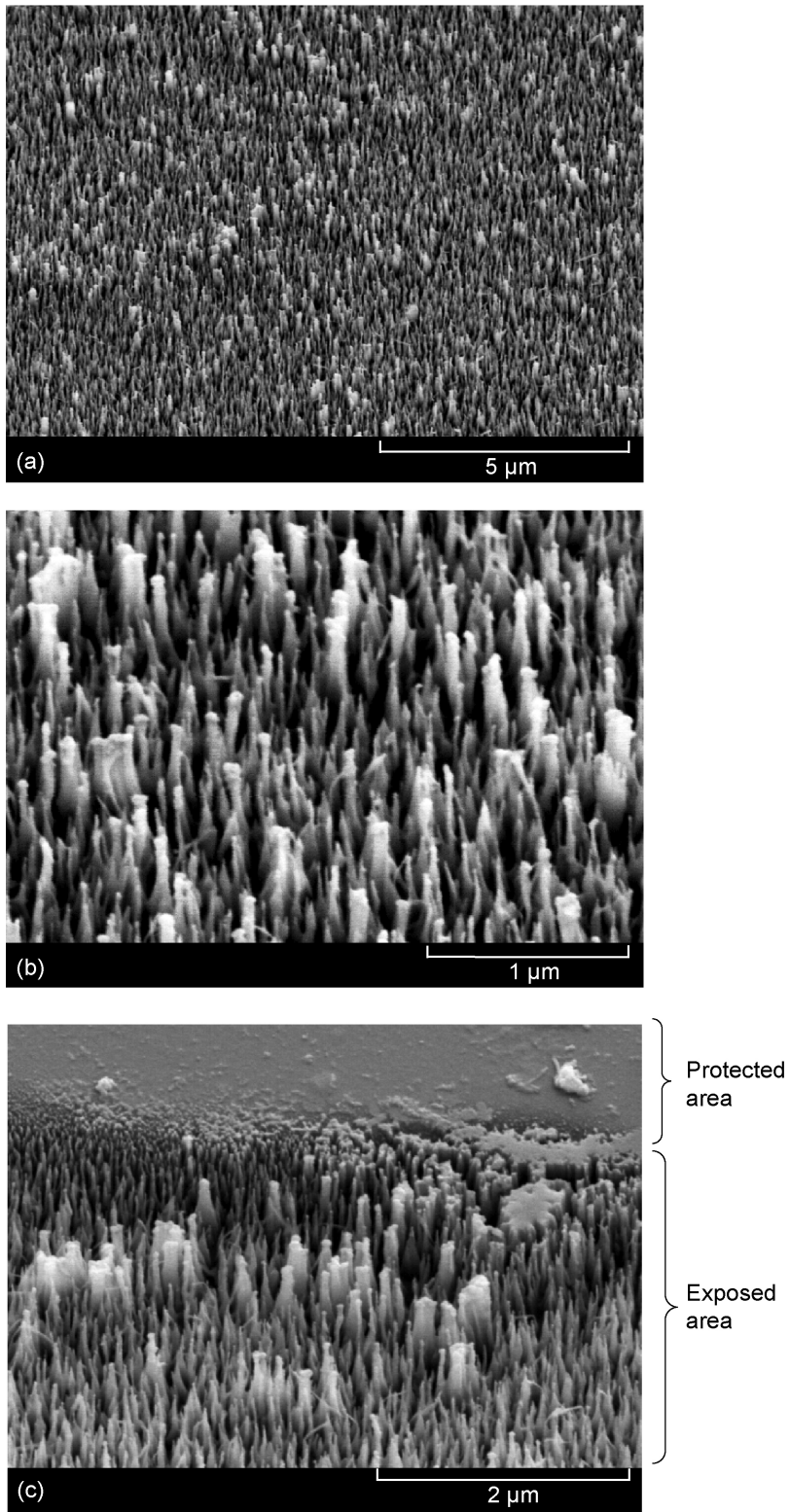cones with residual ash on the tips (1,000×, 45° tilt).

Figure 13.—SEM images (40° tilt) of MISSE 7 AO-eroded diamond.[29]
(a) Image showing AO erosion texture (10,000×). (b) Image of the
AO erosion texture at a higher magnification (40,000×). (c) Image
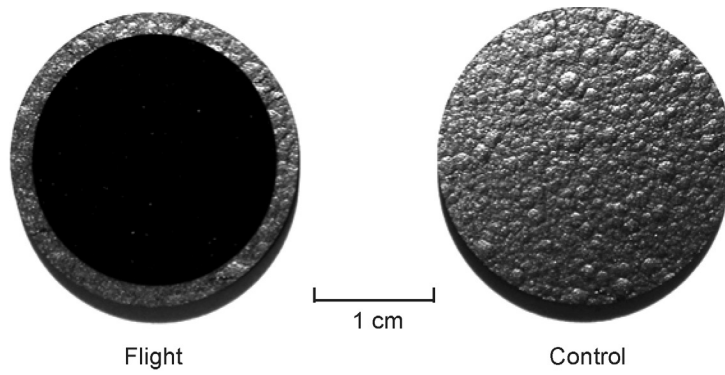of protected (top) and AO-exposed (bottom) border.

Figure 14.—Photograph of MISSE 2 PG flight and control samples.[18]
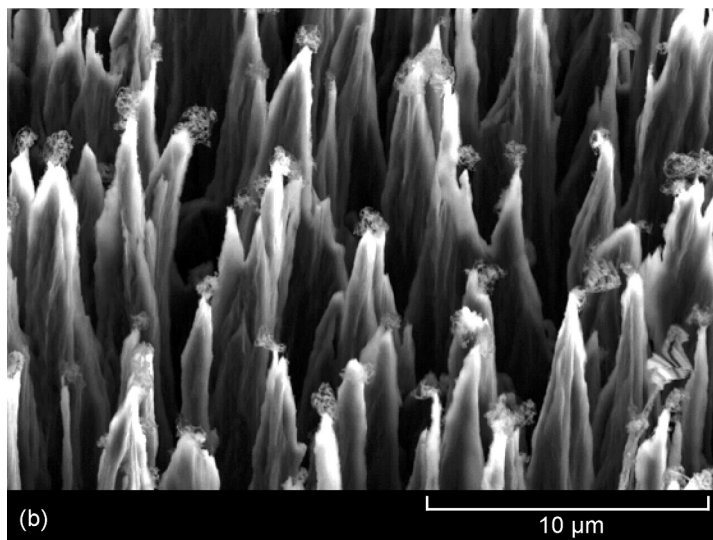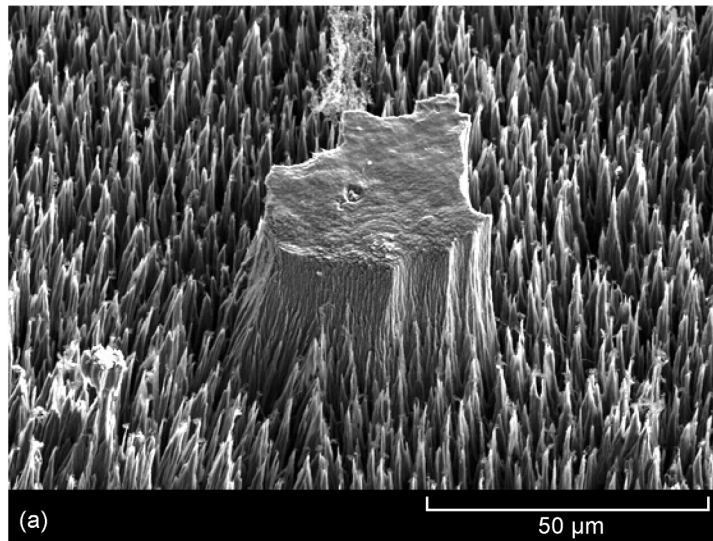
Figure 15.—Erosion texture of MISSE 2 PG.[34] (a) Image at a protected butte showing the total erosion depth (1,000×, 45° tilt). (b) Higher imagination image showing the high-aspect-ratio erosion cones (5,000×, 45° tilt).

The different HOPG planes experienced different levels of erosion and displayed different erosion textures. The MISSE 7 HOPG edge plane had an E_y of $5.38\pm0.90\times10^{-25}$ cm^3/atom and developed directional erosion cones, as shown in Figure 16. The A/D value was 0.557. As can been seen in Figure 16(a), the cross section of the cones resembled elongated parallelograms with longer sections parallel to the edge planes possibly due to the anisotropy of the E_y in the edge versus basal planes. The HOPG basal plane had an E_y of $1.05\pm0.08\times10^{-24}$ cm^3/atom. Thus, the basal plane HOPG eroded 2× as quickly as the edge plane. Figure 17 shows the erosion texture of the HOPG basal plane. The sample was salt sprayed prior to flight to provide isolated protected areas. Figure 17(a) shows erosion around a salt-protected, left-standing "butte." The HOPG basal plane erosion texture seen in Figure 17(b) is not typical of AO erosion of organic materials with volatile oxides. The ratio of texture height to erosion depth for the basal plane was very low (0.016), and typical AO erosion cones were not present even though the material eroded significantly. This ratio is significantly lower than for most polymers and probably indicates that scattering of AO off the edges of HOPG planes causes erosion of any cones that start to form, which results in a reasonably smooth texture.
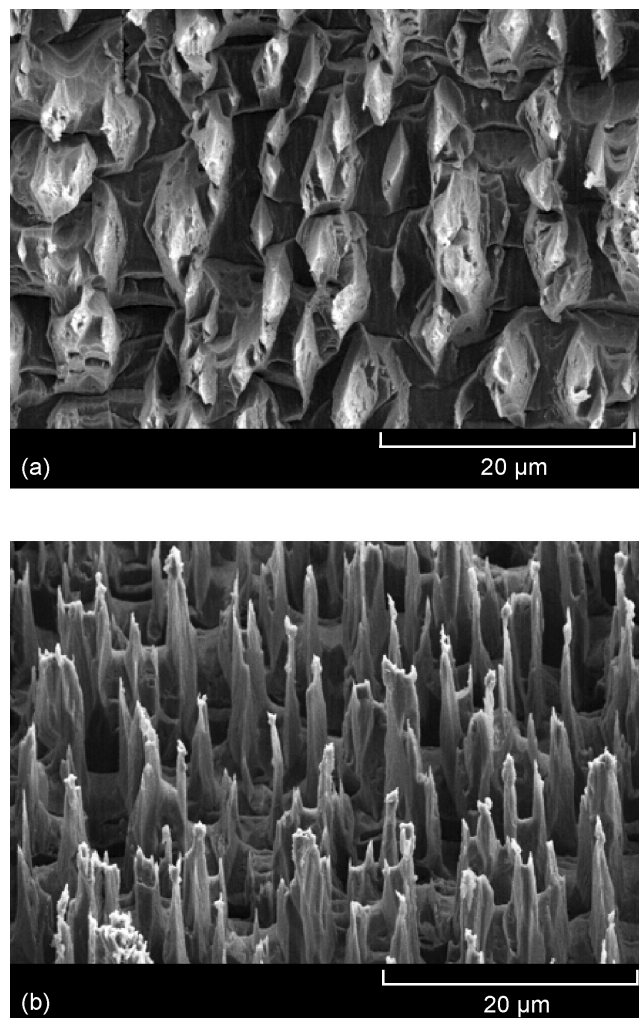

Figure 16.—Erosion morphologies of MISSE 7 HOPG edge plane.[29] (a) 2,500× magnification at 0° tilt. (b) 2,500× magnification at 40° tilt.
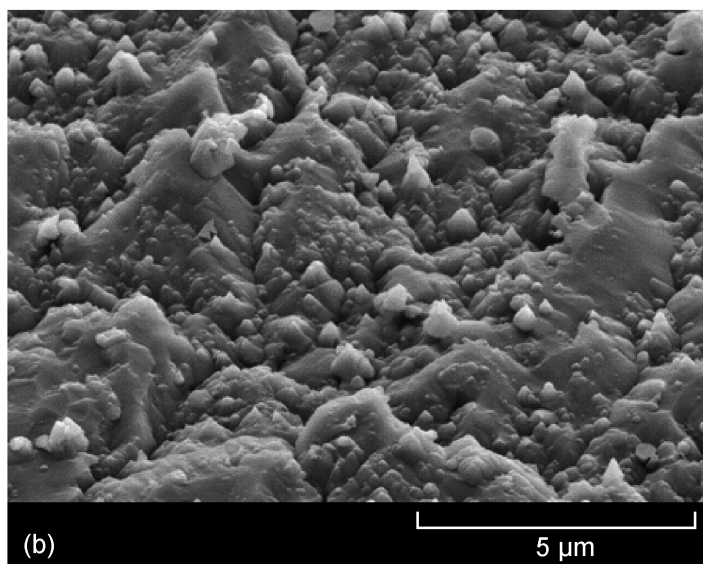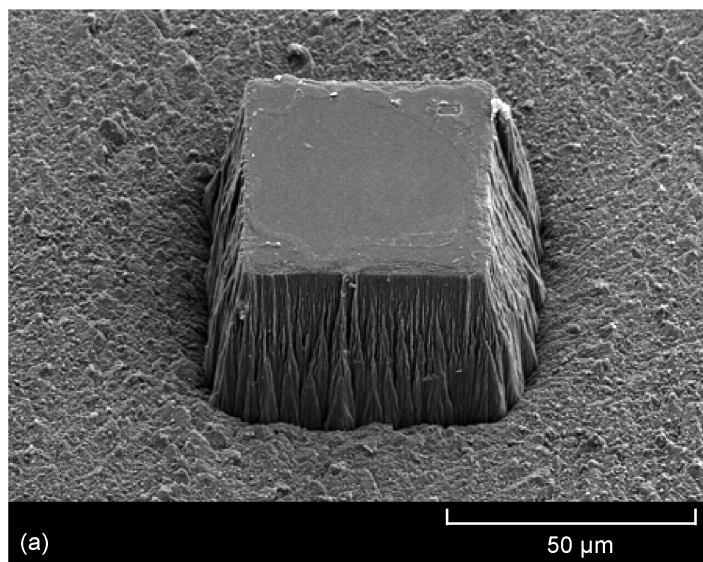
Figure 17.—Erosion morphologies (40° tilt) of HOPG basal plane.[29]
(a) Low-magnification (900×) image at a salt-protected butte.
(b) High-magnification (10,000×) image showing the atypical
erosion texture.

Erosion Dependence on Atomic Oxygen Fluence

White Tedlar® is an example of a material in which the E_y decreases with increasing AO fluence.[22] The E_y for white Tedlar® from three different MISSE missions (MISSE 2, 7, and 8) are plotted versus AO fluence in Figure 18. The decreased E_y with increased AO fluence for white Tedlar® is attributed to a buildup of AO-durable TiO_2 particles on the surface of the samples with increasing AO exposure. The TiO_2 protects the underlying material from erosion if undisturbed, thus decreasing the E_y with increasing AO fluence. Further investigations on the effect of inorganic filler on the AO erosion of polymers and paints are reported by Banks in Reference 15.

Erosion Dependence on Solar Exposure

Prior flight data indicate that the solar exposure (sun hours with corresponding temperature effects, and possibly x-rays) plays a significant role in the erosion of some polymers, with Teflon™ FEP showing a direct correlation.[21,22,35,36] The E_y values for 5-mil-thick Teflon™ FEP from various MISSE missions (2, 4, 6, 7, and 8), the Long Duration Exposure Facility (LDEF), and from space-exposed multilayer insulation retrieved from the Hubble Space Telescope (HST) from servicing mission 2 (SM2) and servicing mission 4 (SM4) are provided in Table 4. Included in the table are the space mission, mission duration, flight orientation, solar exposure, AO fluence and E_y. These E_y values were plotted in numerous ways, including E_y versus AO fluence, time, ESH, and ESH/AO ratio. The best fit was found for E_y versus ESH, and the corresponding graph is shown in Figure 19. As seen in the log-log plot, a simple trend line fit is found for the power law equation $y = 3.24 \times 10^{-29} x^{1.07}$, which has an R^2 coefficient of 0.893.

These data clearly show the effect of solar radiation and/or heating due to solar exposure on FEP erosion. The E_y increased by two orders from 1.28×10^{-25} cm³/atom for the MISSE 4 FEP exposed to 1,400 ESH with an AO fluence of 2.15×10^{21} atoms/cm² to 1.17×10^{-23} cm³/atom for the HST SM4 Bay 8 FEP exposed to 89,300 ESH with an AO fluence of only 4.28×10^{20} atoms/cm². Time likely also plays a role: the HST SM4 FEP was exposed to space for 19 years, but the E_y of the HST SM4 Bay 8 is an order of magnitude greater than the E_y of HST Bay 5 FEP ($E_y = 1.43 \times 10^{-24}$ cm³/atom), also retrieved after 19 years in space, but was exposed to 24,300 ESH and a similar AO fluence (4.28×10^{20} atom/cm²).[36]
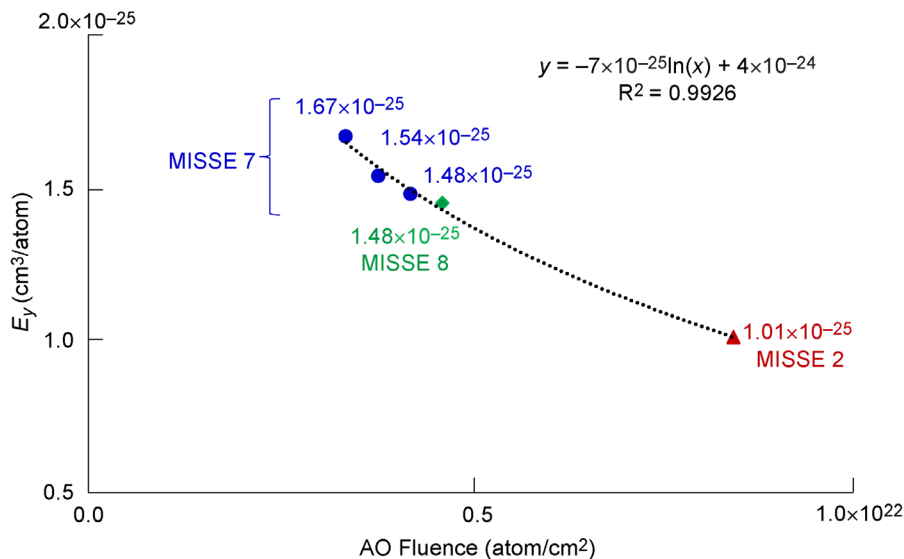

Figure 18.—Erosion yield versus AO fluence for white Tedlar® samples flown on MISSE 2, 7, and 8, showing decreasing E_y with increasing AO fluence.

Table 4. Erosion Yield Values for Teflon™ FEP From Various Flight Missions

| Mission	Material (5 mil)	Flight Orientation	Mission Duration, yr	Solar Exposure, ESH	AO Fluence, atom/cm²	Ey, cm³/atom	Reference
MISSE 4	Ag-FEP	Ram	1.04	1,400	2.15×10^{21}	1.28×10^{-25}	27
MISSE 7	Al-FEP	Ram	1.5	2,400	4.22×10^{21}	1.81×10^{-25}	20, 21
MISSE 6	FEP	Ram	1.45	2,600	1.97×10^{21}	1.69×10^{-25}	19
MISSE 8	Al-FEP	Ram	2	3,200	4.62×10^{21}	2.39×10^{-25}	22
MISSE 2 (E6)	Al-FEP	Ram	3.95	6,100	8.51×10^{21}	2.11×10^{-25}	27
MISSE 2 (E5)	FEP	Ram	3.95	6,300	8.43×10^{21}	2.00×10^{-25}	18
LDEF (Row 9)	Ag-FEP	Ram	5.8	11,160	8.99×10^{21}	3.37×10^{-25}	37
HST SM4 (Bay 5)	Al-FEP	Solar grazing	19	24,300	4.65×10^{20}	1.27×10^{-24}	36
HST SM2	Al-FEP	Sweeping AO	6.8	33,640	3.20×10^{20}	3.10×10^{-24}	38
HST SM4 (Bay 8)	Al-FEP	Sun facing	19	89,300	4.28×10^{20}	1.17×10^{-23}	36
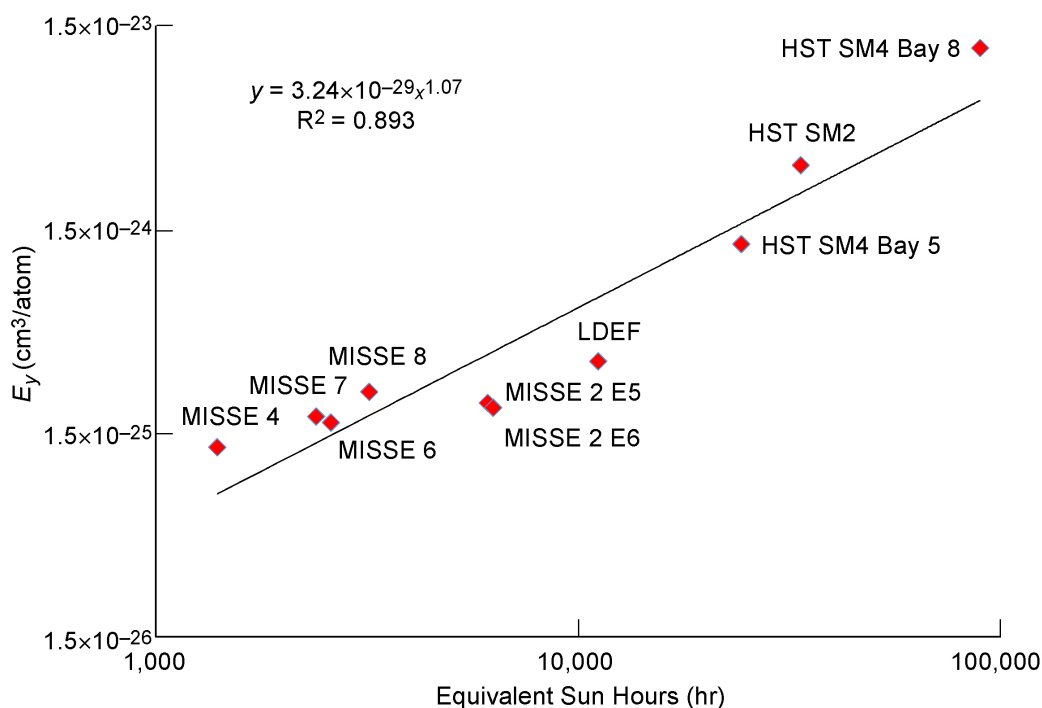
Figure 19.—Erosion yield versus solar exposure (ESH) for Teflon™ FEP flown on various missions.

Summary and Conclusions

Polymers and other oxidizable materials on the exterior of spacecraft in the low Earth orbit (LEO) space environment can be eroded because of reaction with atomic oxygen (AO). Therefore, in order to design durable spacecraft it is important to know the extent of erosion that will occur during a mission. This can be determined by knowing the LEO AO erosion yield (E_y, volume loss per incident oxygen atom) of materials susceptible to AO reaction. In addition, recent flight experiments have shown that the AO E_y can vary with the AO fluence and/or solar exposure. Therefore obtaining AO E_y data for materials flown on various spaceflight missions is important. NASA Glenn Research Center has flown six different passive experiments as part of the MISSE missions with the primary objective of determining the LEO AO E_y of polymers and composites. The experiments were successfully exposed to the space environment on the exterior of the ISS from 1 to 4 years, and retrieved for post-flight analyses. This report provides a compilation of the E_y data for the samples flown in a ram flight orientation. A total of 71 types of materials with 111 E_y values are provided. Seven Kapton® H flight samples, used to determine the mission AO fluence based on a previously characterized LEO E_y (3.0×10^{-24} cm³/atom), are included. Therefore, 104 new E_y values were determined as part of the Glenn MISSE 2–8 polymer flight experiments. Numerous materials were flown on different missions so that trends for E_y versus AO fluence and/or solar exposure can be determined. Polymers with inorganic filler, such as white Tedlar®, are found to have decreasing E_y with increasing AO fluence. Fluoropolymers, such as Teflon™ FEP, are found to have increasing E_y with increasing solar exposure and/or temperature.

Appendix
Trade Names

954-3; HexPly® 954-3 (Hexcel Corporation)
996; HexPly® 996 (Hexcel Corporation)
Absylux® Westlake Plastics Company
Acrylite® ((Evonik Corporation)
Alkox® E-30 powder (Meisei Chemical Works, Ltd.)
Barex® 210 (Ineos Olefins & Polymers USA)
Celazole® PBI 22 (PBI Performance Products, Inc.)
CHEMFILM® DF100 (Saint-Gobain Performance Plastics Corporation)
Clarifoil® Celanese Corporation,
Clear-Lay® (Grafix)
Contour® 28 (GOEX)
CORIN® (NeXolve Corporation)
CP1 (NeXolve Corporation)
CR-39® PPG Industries
Cycolac™, SABIC
DC 93-500 (The Dow Chemical Company)
Delrin® (DuPont)
Dexel (Courtaulds Specialty Plastics)
Dureflex® PS8010 (Covestro LLC)
EX-1515 (TenCate Advanced Composites)
FG-120 fiber glass (DE-COMP Composites, Inc.)
Halar® 300 (Solvay)
Hyflon® MFA® 620 (Solvay S.A.)
Hysol® EA 956 (Henkel Corporation)
Kapton® (E. I. du Pont de Nemours and Company)
Kel-F (3M Company)
Kevlar® (DuPont)
Kynar® 740 (Emco Industrial Plastics, Inc.)
LaRC™ CP1-300 (NeXolve Corporation)
M1000 (MonoSol LLC)
Mylar® A-200, 500 (DuPont Teijin Films)
Neoflon® M-300 (Daikin Industries)
Nomex® (DuPont)
Nomex® Crepe Paper T-410 (DuPont)
PEEREX® 61 (GOEX)
Plexiglas® (Evonik Röhm GmbH)
Teflon®
Tefzel® ZM (DuPont)
Tenite™ Acetate (Eastman Chemical Company)
Thermalux® (Westlake Plastics Co.)
TOR™ LM (Triton Systems, Inc.)
Torayca® M55J (Toray Carbon Fibers America, Inc.)
Torlon® 4203 (Solvay Specialty Polymers, discontinued)
TPX® DX845 Natural (Goodfellow Cambridge Limited)
Trycite™ 1000 (Transcendia, Inc.)
Udel® P-1700 N 11 (Solvay Specialty Polymers)
Ultem™ 1000 (Saudi Basic Industries Corporation)
Upilex®-S (UBE Industries, Ltd.)

VALOX™ 357 (Saudi Basic Industries Corporation)
Vectran™ (Kuraray America, Inc.)
Vespel® (DuPont)
Victrex™ PEEK 450 (Victrex plc.)
White Tedlar® (E. I. du Pont de Nemours and Company)
Zylon® (Toyobo Co., Ltd.)

References

1. Dickerson, Richard E.; Gray, Harry B.; and Haight, Gilbert P.: Chemical Principles. Third ed., Benjamin Cummings Publishing Co. Inc., Menlo Park, CA, 1979, p. 457.
2. de Groh, Kim K.; Banks, Bruce A.; and McCarthy, Catherine E.: Spacecraft Polymers Atomic Oxygen Durability Handbook. NASA–HDBK–6024, 2017.
3. National Aeronautics and Space Administration: U.S. Standard Atmosphere, 1976. NASA TM–X–74335, 1976.
4. Gregory, John C.: Interaction of Hyperthermal Atoms on Surfaces in Orbit: The University of Alabama Experiment. Proceedings of the NASA Workshop on Atomic Oxygen Effects, David E. Brinza, ed., JPL 87–14, 1986, pp. 29–30.
5. Dever, Joyce A.: Low Earth Orbital Atomic Oxygen and Ultraviolet Radiation Effects on Polymers. NASA TM–103711, 1991.
6. de Groh, K.K., et al.: Degradation of Spacecraft Materials. Handbook of Environmental Degradation of Materials, Myer Kutz, ed., Ch. 28, William Andrew Inc., Norwich, NY, 2018, pp. 601–645.
7. O'Neal, Robert L.; Levine, Arlene S.; and Kiser, Carol C.: Photographic Survey of the LDEF Mission. NASA SP–531, 1996.
8. de Groh, Kim K.; and Banks, Bruce A.: Atomic Oxygen Undercutting of Long Duration Exposure Facility Aluminized-Kapton Multilayer Insulation. J. Spacecr. Rockets, vol. 31, no. 4, 1994, pp. 656–664.
9. de Groh, Kim K., et al.: NASA Glenn Research Center's Materials International Space Station Experiments (MISSE 1–7). NASA/TM—2008-215482, 2008.
10. Banks, Bruce A.; de Groh, Kim K.; and Miller, Sharon K.: Low Earth Orbital Atomic Oxygen Interactions With Spacecraft Materials. MRS Symposium Proceedings, vol. 851, NN8.1 (NASA/TM—2004-213400), 2004.
11. Banks, Bruce A., et al.: Sputtered Coatings for Protection of Spacecraft Polymers. Thin Solid Films (NASA TM–83706), vol. 127, 1985, pp. 107–114.
12. Visentine, J.T., et al.: STS–8 Atomic Oxygen Effects Experiment. AIAA 85–0415, 1985.
13. Koontz, Steven L., et al.: EOIM–III Mass Spectrometry and Polymer Chemistry: STS 46, July–August 1992. J. Spacecr. Rockets, vol. 32, no. 3, 1995, pp. 483–495.
14. Silverman, Edward M.: Space Environmental Effects on Spacecraft: LEO Materials Selection Guide. NASA CR–4661, Part 1, 1995.
15. Banks, Bruce A., et al.: The Effect of Ash and Inorganic Pigment Fill on the Atomic Oxygen Erosion of Polymers and Paints. Proceedings of the 12th International Symposium on Materials in the Space Environment (ISMSE 12), ESA SP–705, Noordwijk, The Netherlands, 2013.
16. American Society for Testing and Materials: 2000 ASTM Standard Extraterrestrial Spectrum Reference E–490–00, 2000.
17. de Groh, Kim K.: Materials Spaceflight Experiments. Encyclopedia of Aerospace Engineering, Richard Blockley and Wei Shyy, eds., John Wiley & Sons Ltd., Chichester, 2010, pp. 2535–2552.
18. de Groh, Kim K., et al.: MISSE 2 PEACE Polymers Atomic Oxygen Erosion Experiment on the International Space Station. High Perform. Polym., vol. 20, 2008, pp. 388–409.
19. de Groh, Kim K., et al.: MISSE 6 Stressed Polymers Experiment Atomic Oxygen Erosion Data. Proceedings of the 12th International Symposium on Materials in the Space Environment, ESA SP–705 (NASA/TM—2013-217847), 2013.
20. Yi, Grace T., et al.: Overview of the MISSE 7 Polymers and Zenith Polymers Experiments After 1.5 Years of Space Exposure. Proceedings of the 12th International Symposium on Materials in the Space Environment, ESA SP–705 (NASA/TM—2013-217848 (Corrected Copy)), 2013.
21. de Groh, Kim K., et al.: Erosion Results of the MISSE 7 Polymers Experiment and Zenith Polymers Experiment After 1.5 Years of Space Exposure. NASA/TM—2016-219167 (Corrected Copy), 2016.
22. de Groh, Kim K., et al.: Erosion Results of the MISSE 8 Polymers Experiment After 2 Years of Space Exposure on the International Space Station. NASA/TM—2017-219445, 2017.

23. de Groh, Kim K.; Perry, Bruce A.; and Banks, Bruce A.: Effect of 1.5 Years of Space Exposure on Tensile Properties of Teflon. J. Spacecr. Rockets, vol. 53, no. 6, 2016, pp. 1002–1011.
24. NASA International Space Station Program: ISS Certification Baseline—Volume 3: Flight Attitudes. SSP 50699–03, Rev. B (Incorporates DCN 014), 2008. Available from the NASA International Space Station Program.
25. de Groh, Kim K., et al.: A Sensitive Technique Using Atomic Force Microscopy to Measure the Low Earth Orbit Atomic Oxygen Erosion of Polymers. NASA/TM—2001-211346, 2001.
26. de Groh, Kim K.; Banks, Bruce A.; and Demko, Rikako: Techniques for Measuring Low Earth Orbital Atomic Oxygen Erosion of Polymers. Proceedings of the 2002 Symposium and Exhibition (NASA/TM—2002-211479), 2002, pp. 1279–1292.
27. Dever, Joyce A., et al.: Space Environment Exposure of Polymer Films on the Materials International Space Station Experiment: Results From MISSE 1 and MISSE 2. High Perform. Polym., vol. 20, nos. 4–5, 2008, pp. 371–387.
28. Dever, J.A., et al.: Evaluation of Optical Properties and Atomic Oxygen Erosion Yields of Polymer Film Materials Exposed to the Space Environment on MISSE 3 & 4. Presented at the 2010 National Space and Missile Materials Symposium (NSMMS), Scottsdale, AZ, 2010.
29. de Groh, Kim K.; and Banks, Bruce A.: The Erosion of Diamond and Highly Oriented Pyrolytic Graphite After 1.5 Years of Space Exposure. NASA/TM—2018-219756, 2018.
30. Hung, Ching-cheh; de Groh, Kim K.; and Banks, Bruce A.: Optical and Scanning Electron Microscopy of the Materials International Space Station Experiment (MISSE) Spacecraft Silicone Experiment. Protection of Materials and Structures from the Space Environment, Astrophysics and Space Science Proceedings (NASA/TM—2012-217678), Vol. 32, Springer, New York, NY, 2012, pp. 93–103.
31. Miller, Sharon K.R.; and Dever, Joyce A.: Materials International Space Station Experiment 5 Polymer Film Thermal Control Experiment. J. Spacecr. Rockets, vol. 48, no. 2, 2011, pp. 240–245.
32. Banks, Bruce A., et al.: Atomic Oxygen Erosion Yield Prediction for Spacecraft Polymers in Low Earth Orbit. Presented at the 11th International Symposium on Materials in a Space Environment (NASA/TM—2009-215812), Aix en Provence, France, 2009.
33. Banks, Bruce A., et al.: Comparison of Hyperthermal Ground Laboratory Atomic Oxygen Erosion Yields With Those in Low Earth Orbit. NASA/TM—2013-216613, 2013.
34. de Groh, Kim K.; and Banks, Bruce A.: MISSE 2 PEACE Polymers Erosion Morphology Studies. Presented at the 11th International Symposium on Materials in a Space Environment, Aix-en-Provence, France, 2009.
35. Pippin, H. Gary, et al.: Analysis of Metallized Teflon™ Thin-Film Materials Performances on Satellites. J. Spacecr. Rockets, vol. 41, no. 3, 2004, pp. 322–325.
36. de Groh, Kim K., et al.: Analyses of Hubble Space Telescope Aluminized-Teflon Multilayer Insulation Blankets Retrieved After 19 Years of Space Exposure. NASA/TM—2015-218476, 2015.
37. Banks, B.A.: The Use of Fluoropolymers in Space Applications. Modern Fluoropolymers, Ch. 4, John Scheirs, ed., John Wiley & Sons, Chichester, 1997, pp. 103–113.
38. Dever, Joyce A., et al.: Environmental Exposure Conditions for Teflon Fluorinated Ethylene Propylene on the Hubble Space Telescope. High Perform. Polym., vol. 12, 2000, pp. 125–139.